Fuel Processing Technology 255 (2024) 108064

Contents lists available at ScienceDirect

Fuel Processing Technology

journal homepage: www.elsevier.com/locate/fuproc

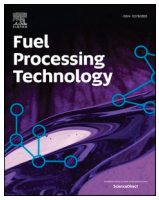

Highly selective catalytic hydrodeoxygenation of guaiacol to benzene in continuous operation mode

J. Gracia [a], A. Ayala-Cortés [a], C. Di Stasi [a], J. Remón [a,b], D. Torres [a], J.L. Pinilla [a,*], I. Suelves [a]

[a] Instituto de Carboquímica, CSIC, C/ Miguel Luesma Castán, 4, 50018 Zaragoza, Spain
[b] Thermochemical Processes Group, Aragón Institute for Engineering Research (I3A), University of Zaragoza, C/Mariano Esquillor s/n, 50.018 Zaragoza, Spain

ARTICLE INFO

Keywords:
Catalytic hydrodeoxygenation
Guaiacol upgrading
Benzene production
Continuous reactor

ABSTRACT

Benzene, mostly produced from fossil fuel sources, is an essential chemical to many modern industries. Alternatively to non-renewable methods currently used, the present work explores using fast pyrolysis biomass-derived bio-oils to furnish this valuable platform molecule. Notably, we report for the first time the impact of different operational parameters on the highly selective continuous catalytic hydrodeoxygenation of guaiacol, a bio-oil model compound, into benzene using a Mo_2C/CNF-based catalyst. The parametric study includes a first evaluation of the effect of the hydrogen pressure (25, 50 and 75 bar), temperature (300, 325 and 350 °C) and weight hourly space velocity (4 and 10 $g_{org}\ g_{cat}^{-1}\ h^{-1}$) on the guaiacol conversion and product distribution, and a subsequent long-term evaluation (30 h on stream) of the catalyst under appropriate processing conditions The experimental results revelated that our Mo_2C/CNF was able to achieve a conversion of 90–98% with a relative amount of benzene in the liquid product up to 81% for at least 30 h without any sign of deactivation at 75 bar of H_2 and 350 °C, which is a landmark achievement in the conversion of bio-oil derived molecules into platform chemicals.

1. Introduction

Benzene (C_6H_6) is a base compound of aromatic organic chemistry. It is a volatile hydrocarbon and solvent with thermal stability, also classified as a carcinogen. In spite of the environmental and health issues that its use leads to, it is an essential chemical used widely in many industries, for instance, in gasoline blending as a result of its high octane value, and many other industries in which is part are detergents, plastics, paint and dyes [1]. Its primary use in modern society is as a fundamental building block to produce platform chemicals, such as ethylbenzene, cumene and cyclohexane, and then styrene, phenol, aniline and alkylbenzenes. These substances are fundamental to manufacturing polystyrene plastics, resins, nylon and detergents.

Benzene production increased after the decade of 1950 since the industrial development and world population led to higher consumption. Moreover, current-year production is around 37 million tons, and it is expected to keep increasing by 3.8% per year [2,3]. However, around 90% of the global chemical requirements comes from fossil fuel sources, such as natural gas and naphtha [4]. Consequently, it is vital to reduce dependence on fossil fuel sources and be more aware of the environmental impacts of using non-renewable energy sources. Given this energy picture, biomass has emerged as a promising source of electricity, fuels and chemicals because it is an abundant, widely available, low-cost, and carbon-neutral energy source [5]. However, biomass has low energy density and requires further treatments to increase its properties and be suitable for fuel or chemical use. On the bright side, thermochemical biomass conversion processes are well-studied methods to transform biomass into a variety of solid carbonaceous, bio-oil, and gas fuels [6–8]. Among these, fast pyrolysis is one of the most promising and mature thermochemical processes to convert solid biomass into a high-energy density liquid called *bio-oil* {Di Stasi, 2021 #156;Di Stasi, 2021 #155;Di Stasi, 2019 #157} [9–12].

Nevertheless, the obtained bio-oil presents some physicochemical properties that complicate its direct application. Some of the main characteristics associated with bio-oils are high viscosity, elevated volatility, acidity, corrosiveness, and high moisture content (depending on the feedstock and the operating conditions). All these properties lower the heating value of the biofuel and increase its thermal instability, causing aging problems and transport/storage issues [13–15]. These concerns are mostly related to the presence of oxygenated organic compounds, such as acids, alcohols, aldehydes, esters, ketones and lignin-derived phenols [16]. Therefore, an upgrading process is needed

* Corresponding author.
E-mail address: jlpinilla@icb.csic.es (J.L. Pinilla).

https://doi.org/10.1016/j.fuproc.2024.108064
Received 24 November 2023; Received in revised form 12 February 2024; Accepted 16 February 2024
Available online 21 February 2024
0378-3820/© 2024 The Authors. Published by Elsevier B.V. This is an open access article under the CC BY-NC license (http://creativecommons.org/licenses/by-nc/4.0/).

to remove these compounds and convert the bio-oil into a suitable chemical.

Catalytic hydrodeoxygenation (HDO) is a method for the removal of oxygen heteroatoms [17]. HDO is usually carried out at operational temperatures and pressures of 250–500 °C and 20–300 bar in a highly rich hydrogen atmosphere [18–21]. The main goal of the HDO process is to remove the oxygen present in the bio-oil through decarboxylation, decarbonylation, dehydration and hydrogenolysis reactions, in which hydrogen reacts with the oxygen over the catalyst to produce mainly water, CO_2, CO and an upgraded bio-oil [22]. As previously mentioned, bio-oil is a complex mixture of many compounds and different organic groups, complicating the identification of the analysis and reaction pathways. Therefore, the use of model compounds with properties similar to those of bio-oil is a common strategy that allows for a better understanding of the reaction mechanism [23]. In this context, guaiacol, $C_6H_4(OH)(OCH_3)$, is a molecule obtained by the thermal decomposition of lignin [24–26], and it is usually considered a representative model compound of bio-oil phenolic groups from fast pyrolysis [27–29] and, therefore, can contribute to clarifying the reaction mechanism that bio-oil follows through HDO treatment.

During recent years, the interest in the catalytic HDO of guaiacol has significantly increased, especially in catalyst development. Noble metals such as Pt and Pd [30] are known for their high performance, stability, and active sites. Nevertheless, their elevated cost and scarce availability make them an expensive option for the processing of low-value biomass-derived compounds. Transition metals such as Mo, Ni, Nb, V and W are considered valid alternatives to noble metal-based catalysts. In particular, Co-MoS_2/Al_2O_3 and Ni-MoS_2/Al_2O_3 [31–34] are considered conventional catalysts in the HDO. However, the main drawback associated with their employment is the catalytic deactivation caused by the transformation of the alumina phase into boehmite as a consequence of water presence. Additionally, the acidity of alumina may promote coke formation, which leads to catalyst deactivation.

Furthermore, considering that the above-mentioned catalysts are sulfidated, sulfur compounds may be migrated from the catalyst to the bio-oil, which leads to contaminating the upgraded fuel with undesirable sulfur species [35–38]. Recently, numerous works focused their attention on the study of novel catalysts based on transition metal carbides due to their exceptional catalyst properties [39–42] and relatively better availability with respect to noble metals. The main advantage of such carbides is the solid electronic interaction between the carbon and the metal, which gives carbides peculiar electronic properties [36]. Furthermore, due to their catalytic properties, carbides of Mo and W are usually referred to as having a “Pt-like behavior”, which makes them have a remarkable activity toward reactions that involve the cleavage of the C—O bond (e.g., hydrogenolysis, hydrogenation or isomerization) [37,38].

Carbon support materials are attractive for being the carbon source for carburization during the carbothermal hydrogen reduction of catalyst salts. At the same time, hydrogen acts as the carburization agent. The efficiency of these supported carbides is, in most cases, higher than that of bulk molybdenum carbide as a result of the enhanced availability of the active sites, resulting from greater dispersion of the carbide phases in the carbon supports [43]. During HDO, H_2 consumption can be reduced due to their high efficiency in oxygen removal [44]. As a result, different carbon supports have been analyzed, including activated carbon (AC), reduced graphene oxide (RGO), carbon nanotubes (CNT), and carbon nanofibers (CNF), in the formation of a Mo_2C catalyst by carbothermal hydrogen reduction, and tested in the hydrodeoxygenation of guaiacol. It was found that CNF as a support material achieved the highest conversion and liquid product distribution into cyclohexane, phenol, and benzene, which was ascribed to higher thermal stability and reduced gasification reactions [45].

Previous publications [39–41,46,47] have analyzed the hydrodeoxygenation of guaiacol in a continuous reactor using different monometallic and bimetallic catalysts such as Co, Fe, Pd—Co, Pd—Fe, Pt/C, Pd/C, Rh/C, Ru/C, NiMo with an emphasis in catalyst deactivation and regeneration [39,40] while other studies focus in the partial or fully deoxygenation of guaiacol into chemicals such as phenol, cyclohexane, anisole and benzene [41,46,48]. Among the catalysts able to fully deoxygenate guaiacol into benzene, various selectivities are reported, wherein values up to 63% were attained with a Ni-Al_2O_3 based catalyst [41], 25% NiMo [49], 70% β-Mo_2C [48], 74% Mo_2C [49] and 63% MoWC [50]. For this reason, Mo_2C appears to be an attractive catalyst for benzene production from the HDO of guaiacol. However, to the best of the authors' knowledge, a parametric study that analyzes the impact of the reactor conditions during the conversion of guaiacol into benzene, and the long-term catalytic behavior of Mo_2C-based catalysts in continuous mode has not yet been reported.

Considering this research opportunity, the present work addresses the performance evaluation of a Mo_2C/CNF catalyst during the HDO of guaiacol for the highly selective benzene production in a continuous trickle-bed reactor, with the influences of the main operational parameters being analyzed in depth. Given the lack of work using continuous-flow reactors for the HDO of bio-oils in general, or guaiacol in particular, this work represents a step ahead toward moving from lab-based batch reactors to industrial continuous-flow reactors, boosting the short-term future development of this technology for fuel and platform chemical production.

2. Experimental

2.1. Materials and catalyst synthesis

The catalyst employed was based on Mo_2C nanoparticles supported on carbon nanofibers (Mo_2C/CNF), whose preparation procedure was optimized in previous work [44,51]. Likewise, the exhaustive physicochemical characterization of the 10 wt% Mo loading catalyst can be found elsewhere [44]. Briefly, the catalyst preparation can be resumed in three main steps: i) CNF preparation; ii) CNF impregnation with the Mo precursor salt; and iii) carbothermal hydrogen reduction (CHR), also referred to as the carburization process. Firstly, carbon nanofibers (CNF) were synthesized by synthetic biogas decomposition (CH_4: CO_2; 50:50 *v/v*) over a Ni:Co:Al catalyst (33,5:33,5:33; wt%) in a rotatory bed reactor at 650 °C using a weight hourly space velocity of 30 STP L g_{cat}^{-1} h^{-1} [52]. Before impregnating the metal salt, CNF were treated with hydrochloric acid (37%, PA-ACS-ISO, FLUKA) at 60 °C in an ultrasonic bath for 4 h in order to remove the metal catalyst used for its synthesis [23]. CNF were further treated with nitric acid (65%, PA-ISO, PANREAC) at its boiling temperature for 1 h. This treatment ensures the creation of oxygenated groups on the catalyst surface, facilitating the subsequent molybdenum impregnation and dispersion. After each treatment, CNF were filtered and rinsed with deionized water until a neutral pH was reached. Finally, the CNF were dried overnight at a mild temperature (85 °C).

The Mo_2C/CNF catalyst was prepared by incipient wetness impregnation of the acid-treated CNF (molybdenum nominal loading: 10 wt%) with an aqueous solution of ammonium heptamolybdate tetrahydrate $(NH_4)_6Mo_7O_{24}{\cdot}4H_2O$ (99.98% Sigma-Aldrich) followed by a carbothermal hydrogen reduction. This latter step was carried out “in-situ” in the reactor prior to the HDO process. During this step, the impregnated catalyst precursor was heated under a H_2 atmosphere (50 NmL g^{-1}) to 750 °C using two different ramps: 10 °C min^{-1} until 350 °C and then 1 °C min^{-1} until the final temperature to produce the active catalyst. The final temperature was held for 1 h; afterward, the sample was cooled down with N_2. After reaching the experimental temperature, the feed was shifted again to H_2 and the catalytic test immediately started. Before using our Mo_2C/CNF catalyst in the continuous flow reactor, it was tested over different carboreduction conditions to improve its catalytic activity [44]. Additionally, it was evaluated in discontinuous systems with model compounds and real bio-oils to prove its catalytic activity, including some control experiments to prove that the addition of the catalyst supports the hydrodeoxygenation reactions [53,54].

2.2. Catalyst characterization

X-ray diffraction (XRD) was conducted on a Bruker D8 Advance Series 2 diffractometer equipped with Ni-filtered CuKα radiation and a secondary graphite monochromator to analyze the crystallite size, phase composition, and structure of the final catalyst. The scans were performed using a range of 20–80° each 0.05° every 3 s. The crystal size was processed using DIFRAC PLUS EVA 8.0 and TOPAS software. The metal composition of the catalyst was obtained by inductively coupled plasma optical emission spectrometry (ICP-EOS); the sample was prepared by sodium peroxide fusion procedure and introduced to Spectroblue (AMETEK) for the quantification. X-ray photoelectron spectroscopy (XPS) patterns were obtained in an ESCAPlus (OMICROM) spectrometer equipped with a hemispherical electron energy analyzer. X-ray was operated at 225 W (15 mA and 15 KV) using a non-monochromatized MgAlα (hυ = 1486.7 eV) under vacuum (<5 × 10–9 Torr). CASA XPS software performed deconvolutions and processing of XPS spectra using Shirley-type background, peak fitting, identification and quantification.

2.3. HDO experimental procedure

The HDO experiments were carried out in a fixed bed reactor operating in a trickle bed regime (Fig. 1). The fixed bed reactor used was made of 316 L stainless steel with a length and inner diameter of 24 cm and 9 mm, respectively.

For each test, 1.5 g of Mo-impregnated CNF was mixed with 4.0 g of an inert material (SiC) to prevent heat losses and gas bypass and ensure that the reaction volume remained constant. The solid mixture was placed over a metal grid located in the middle of the reactor tube and sandwiched with glass wool to prevent losses due to entrainment phenomena. The liquid phase fed to the reactor was a mixture of 5 vol% of guaiacol (99 vol%, Sigma Aldrich) in decane (95 vol%, Sigma Aldrich). The reaction product mixture was cooled down in a counter-flow heat exchanger to ensure the condensation of the products, which were finally separated in a phase separation unit, allowing the sampling of liquid and gas aliquots.

The catalytic tests were carried out under different conditions of temperature, pressure and weight hourly space velocity (*WHSV*, Eq. (1)) to establish the optimal operating conditions in terms of guaiacol conversion and desired product distribution.

All the liquid aliquots collected throughout the reaction were filtered using a 20 μm filter syringe before their analysis to remove any traces of the catalyst. The liquid products were analyzed by gas chromatography, CLASUS 5080 Perkin Elmer, coupled with an FID detector to determine their composition. As described elsewhere, unreacted guaiacol and liquid products were identified and quantified [55].

The guaiacol conversion (X) and the product distribution ($Product_{distrib.}$) were calculated according to Eqs. (2) and (3), respectively, with an experimental error (determined by the repetition of experiments at identical processing conditions) below 5%. The analysis of the experimental error, as error bars, is shown for the most representative experiments (Fig. 5), which are those exploring the stability of the catalyst at different space velocities. The variations observed in this work are more marked than the experimental error, which makes it possible to distinguish between the effect of a variable and the inherent experimental error. In these equations, w_i *and* w_g represent the mass flow rate of the i-component and guaiacol, respectively; while n_i and n_g are the molar flow rates of the i-component and guaiacol, respectively.

$$WHSV\left(\frac{g_{org}}{g_{cat}\,h}\right)=\frac{w_{g\ IN}}{m_{cat}}\times 100 \tag{1}$$

$$X\ (\%)=\frac{n_{g\ IN}-n_{g\ OUT}}{n_{g\ IN}}\times 100 \tag{2}$$

$$Product_{distrib.}\ (\%)=\frac{w_{i\ OUT}}{w_{g\ IN}-w_{g\ OUT}}\times 100 \tag{3}$$

3. Results

3.1. HDO of guaiacol

Removing the oxygen atoms from guaiacol is a complex process involving several reactions in series and/or parallel. A schematic overview of the different reaction pathways of hydrodeoxygenation of

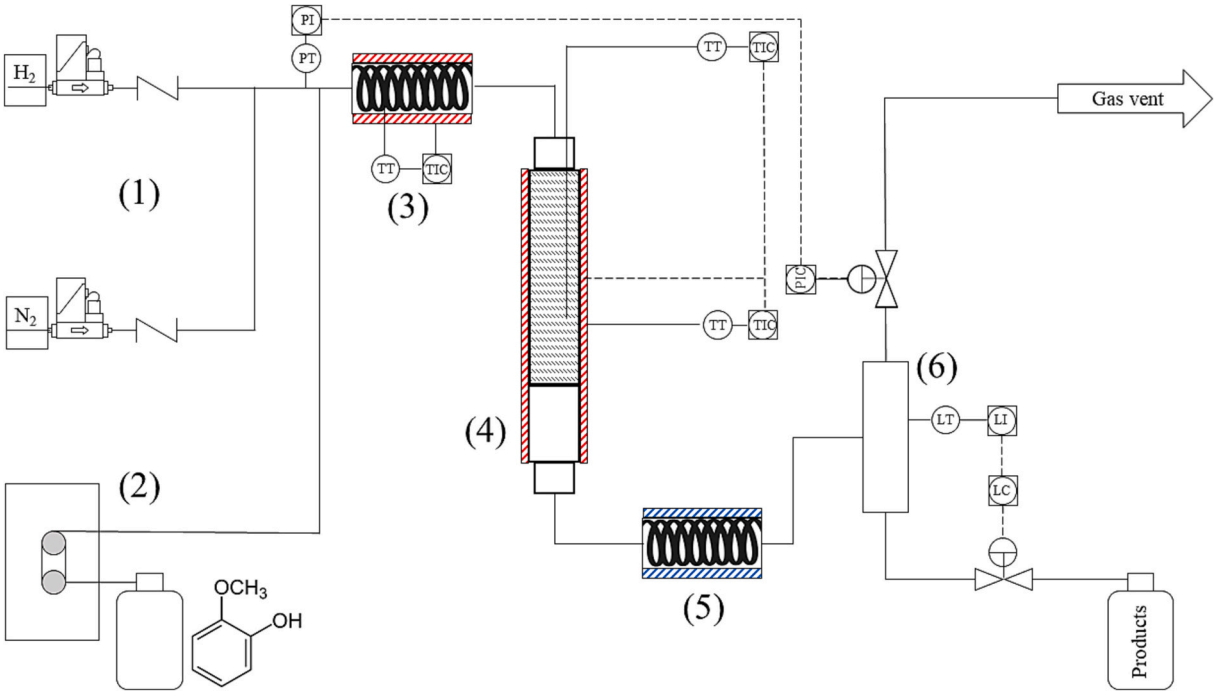

Fig. 1. Scheme of the unit used on the HDO run test: (1) Gas feeding system; (2) Liquid feeding system; (3) Pre-heater; (4) Reactor; (5) Counter-flow heat exchanger; (6) Phases separator.

guaiacol, adapted from our previous work [53], is given in Fig. 2.

Depending on the number of removed oxygen atoms, it is possible to categorize the products into four groups: when no oxygen is removed from the guaiacol, but there is a loss of a methyl group, the resulting molecule is the catechol; if one oxygen is removed, phenol, anisole and o-cresol are produced; when the two oxygens of guaiacol are removed, the products are toluene, benzene or cyclohexane; in all scenarios, the intermediate products may undergo condensation/oligomerization reactions, producing high molecular weight compounds (e.g., Oligomers) which are soluble in the liquid phase but are not detectable by gas chromatography [56]. Therefore, in this work, the content of oligomers (defined as "other") was quantified by the difference in mass balance. Moreover, the amount of "others" (mainly soluble oligomers and condensation products not detected by GC), initially accounting for >60% of the products, practically disappeared. This indicates that these products are mostly formed at relatively high conversion values.

3.2. Influence of the H_2 pressure

Three different hydrogen pressures (25, 50 and 75 bar) were tested at 300 °C and a WHSV of 4 $g_{org}\ g_{cat}^{-1}\ h^{-1}$ to study the influence of pressure on the catalyst activity. It must be borne in mind that an increase in H_2 pressure always supposes an increase in both H_2 partial and total pressure.

The resulting conversion curves through time (Fig. 3) show that the increase in H_2 pressure had beneficial effects on the catalytic stability and desired product distribution. The experiment performed at 25 bar showed lower catalyst stability than the one performed at 50 bar. In fact, even though the conversion obtained during the first 30 min of both experiments was equal to 80%, it is possible to observe a completely different behavior throughout the reaction time. When the experiment was carried out at the lowest H_2 pressure, the activity of the catalyst sharply decreased during the first hour, halving its original value after 6

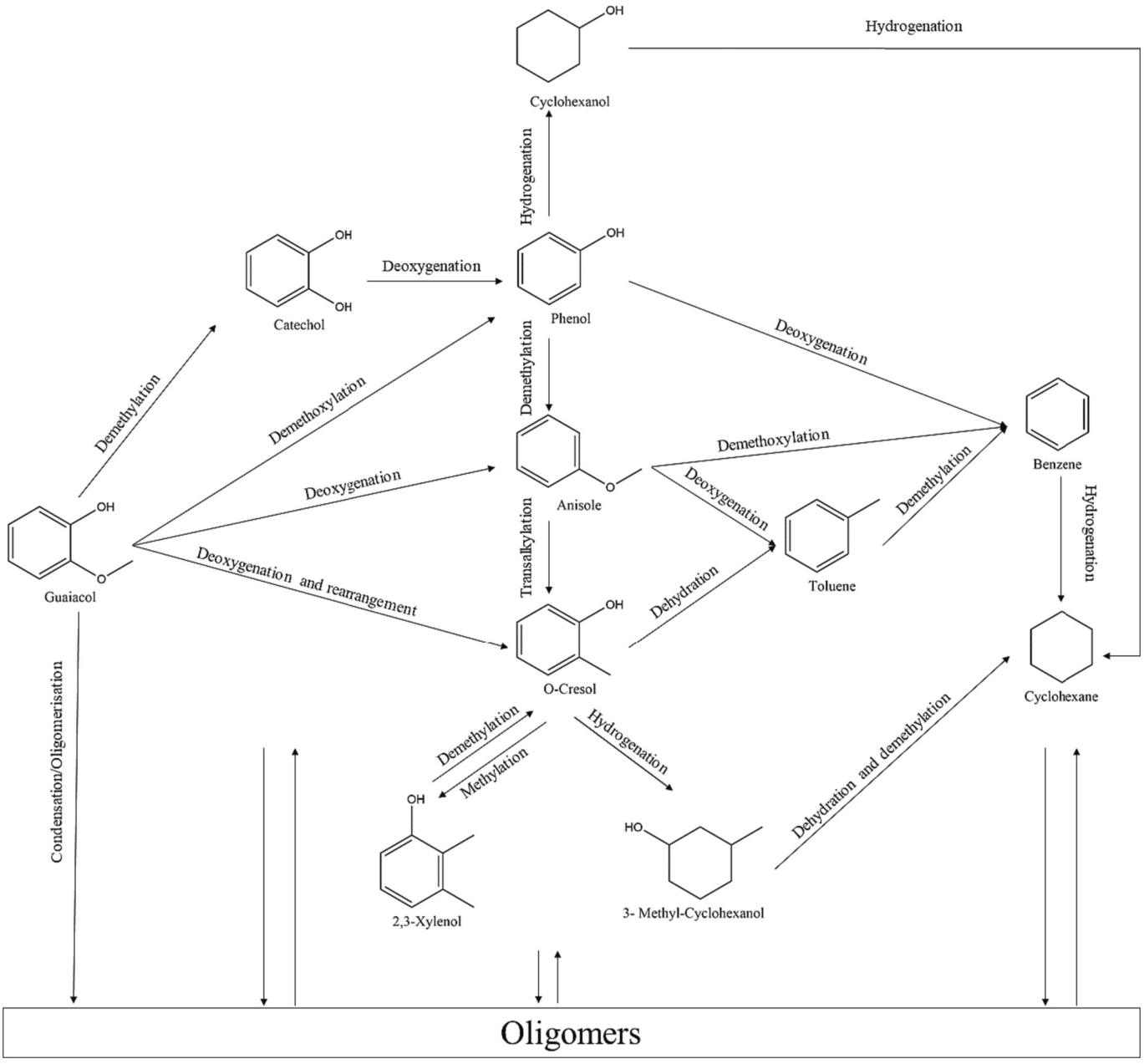

Fig. 2. Reactions occurring during the HDO of guaiacol [53]. Reprinted (adapted) from publication Remón et al. "Towards a sustainable bio-fuels production from lignocellulosic bio-oils: Influence of operating conditions on the hydrodeoxygenation of guaiacol over a Mo_2C/CNF catalyst".

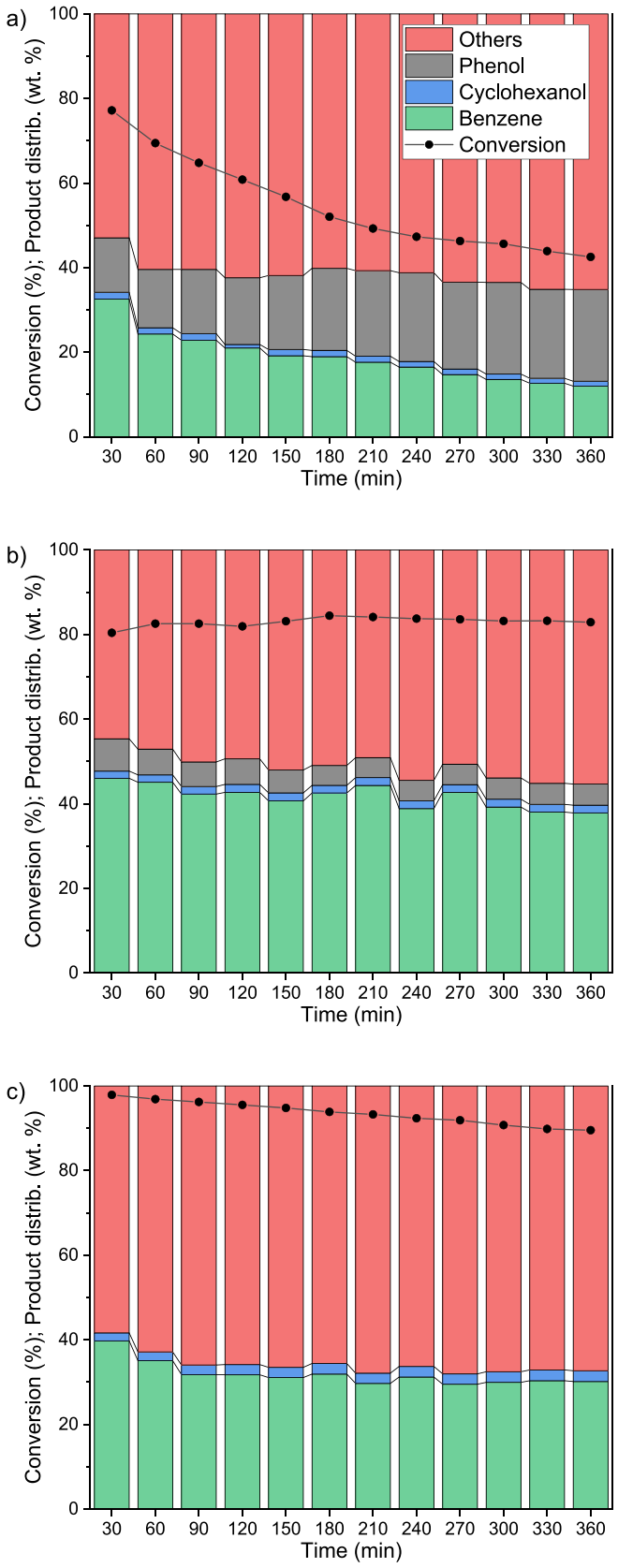

Fig. 3. Conversions and product distribution obtained in the HDO of guaiacol at 300 °C for a WHSV of 4 g_{org} g_{cat}^{-1} h^{-1} and a) 25, b) 50 and c) 75 bar of H_2 pressure.

h. On the contrary, 50 bar of H_2 seemed high enough to maintain the catalyst active during the whole duration of the experiment and keep the benzene production in the range of 40–45%, double the value obtained during the test at 25 bar. This increase in benzene production was accompanied by a decrease in the content of intermediate products, such as phenol, which were reduced by half. This suggests that at 25 bar, the shortage of dissolved hydrogen available for the reaction could lead to an incomplete conversion of guaiacol into products. This behavior was previously reported by Han et al. [28], who also investigated the effect of the H_2 pressure on the reaction mechanism. They found that, depending on the hydrogen availability, the guaiacol conversion may follow two different routes: the phenol route and the 2-methoxycyclohexanol pathway. Both routes lead to the production of cyclohexane, involving the production of phenol or 2-methoxycyclohexanol as the reaction intermediate, respectively. Hence, higher pressures are needed to promote the targeted product formation to ensure the proper amount of dissolved hydrogen in the liquid.

This hypothesis was confirmed by a further increase in H_2 pressure to 75 bar, which resulted in a relatively stable catalytic activity (10% conversion loss after 6 h reaction time) and a complete disappearance of phenol accompanied by a decrease in benzene production and an increase of oligomers. As previously mentioned, these oligomers are usually generated by the condensation reactions of guaiacol and/or other intermediate products. Therefore, the results obtained in Fig. 3c may suggest that an increase in the H_2 pressure promotes the condensation reactions of guaiacol and/or phenol, hindering their conversion toward HDO products. This latter observation can be ascribed to the competition between aromatic hydrogenation and condensation.

Bearing in mind that the three experiments were carried out under the same temperature, and that the Tamman temperature (defined as half of the melting temperature) of Mo_2C is higher than the one of metallic Mo (1169 °C) [56,57], it is unlikely that sintering was involved in the deactivation mechanism. Therefore, the loss in activity shown in Fig. 3, which also resulted in a decrease in the conversion of phenol toward benzene, was probably caused by catalyst poisoning by hardly-desorbable compounds such as condensed aromatic rings and/or other phenolic compounds [40,58] or by coke deposition. Another possibility is represented by the catalyst poisoning by the strong oxygen binding to Mo_2C, allowed by the lack of H_2 [58].

According to the distribution of the products in Fig. 3, it can be seen that the Mo_2C/CNF catalyst promoted the deoxygenation of guaiacol more substantially than its hydrogenation to cyclohexane, which might open a future research window into valuable aromatic chemicals production. The same results were obtained by Liu et al. [59], who observed that when noble metals catalysts were employed, cyclohexane was the main product; meanwhile, our Mo_2C catalyst was not able to hydrogenate the aromatic ring completely. This phenomenon could be ascribed to the elevated oxidation degree [44] (i.e., high Brønsted acidity) of the catalyst that caused a decrease in the hydrogenation reaction rate (occurring on the metallic sites) and hindering the hydrogenation of the aromatic ring [60].

Considering the stability of the catalyst during the two experiments at the higher pressures and the respective product distributions attained at such pressures, it could be stated that the presence of phenols at 50 bar was due to a lack of hydrogen availability, which was remedied by the increase in the H_2 pressure. To summarize, the higher the pressures employed, the better the conversion and product distribution results, primarily due to the higher conversion rates achieved and the lack of intermediate compounds. For this purpose, the following experiments were carried out at 75 bar. By comparing Fig. 3b with Fig. 3c, it can be seen that the liquid product obtained at 50 bar contained a higher proportion of benzene (46 wt%) than at 75 bar (40 wt%). In parallel, such an increase in the H_2 pressure augmented the guaiacol conversion from 80 to 98%. However, the variation observed in the guaiacol conversion is more pronounced than that observed for the relative amount of benzene in the liquid, which overall results in an increase in benzene

production with increasing the H_2 pressure, not to mention the higher stability over time observed for higher pressures. For example, taking benzene production as the binomial formed by guaiacol conversion and benzene proportion in the liquid,

for Fig. 3b, the final quantity of benzene at 30 min is around 36.8 wt %; meanwhile, in Fig. 3c it is 39.2 wt%. This development suggests two things: i) benzene production increased after increasing the H_2 pressure, and/or ii) the reduction in the relative amount of benzene is attributed to the additional species that appeared by increasing the guaiacol conversion due to a superior H_2 pressure. These species might be products of phenol conversion into the group of "others" as intermediate species during the hydrodeoxygenation into benzene.

3.3. Influence of the operating temperature

Three different temperatures, 300, 325 and 350 °C, have been tested to improve the catalyst product distribution toward the relative amount of benzene in the final liquid. From Fig. 4, it is possible to observe that an increase in temperature from 300 °C to 325 °C and 350 °C had a positive effect on the conversion of guaiacol, which ranged from 90% (at the lowest temperature) to 100% (at the highest temperature). At temperatures of 325 and 350 °C, the increase in conversion was accompanied by a notable enhancement in catalyst stability, as evidenced by the absence of any deactivation signs even after 360 min on stream. Even though an increase of 25 °C slightly affected the overall catalytic performances, increasing guaiacol conversion and catalyst stability, the distribution of the products was shifted toward the obtention of benzene at the expense of oligomers.

By comparing the results obtained at 325 and 350 °C, a slight improvement in the distribution of products can be observed, increasing the desired product content by 10%. So, the temperature positively affects the reaction by promoting the complete hydrodeoxygenation of guaiacol and avoiding the non-catalytic reactions that may form higher-weight compounds. Furthermore, the stability of the catalyst improved, showing no deactivation signs during the whole experiment. To summarize, the higher the temperature used, the better conversion and product distribution results. As a consequence, the next experiments were carried out at 350 °C.

Previous authors have analyzed the effect of temperature on the guaiacol conversion and the liquid product distribution. For instance, Tran et al. (2019) [61] employed a continuous reactor for the HDO of a solution of 5 wt% guaiacol/decane over a Mo_2C based-catalyst and evaluated the effect of temperature from 250 to 350 °C. They reported an increasing trend in the guaiacol conversion (up to 80%) with temperature and reached benzene selectivity values of up to 40 mol%. In another work, Lin et al. (2011) [62] examined noble metal catalysts on the HDO of guaiacol. These included Rh, PtRh, and PdRh, which showed high conversions (between 80 and 100%) at different temperatures (300, 350, and 400 °C). Moreover, the liquid product species at 300 °C showed a higher presence of double oxygenated compounds, whose relative amount in the product reduced as temperature increased up to 400 °C to form compounds with one atom of O. Nevertheless, the dominant compound with temperature was cyclohexane, which suggested that intermediate species during the demethylation and hydrogenation of guaiacol, such as benzene and cyclohexene, are suppressed.

The reaction mechanism during HDO of guaiacol has been previously proposed by different authors [53,63,64]. Remón et al. (2019) [53] suggested a possible reaction pathway considering the stages in which guaiacol reacts from partial to complete deoxygenation. For instance, guaiacol may first react through demethylation to form catechol without presenting any deoxygenation. With further reactions of deoxygenation, such as demethoxylation, rearrangement, transalkilation, demethylation, and hydrogenation, some chemicals, including one oxygen atom on their structures, such as phenol, anisole, o-cresol, 2,3-xylenol, and 3-methyl-cyclohexanol, can be produced. One of the final deoxygenated products that might be produced is toluene, which, after demethylation,

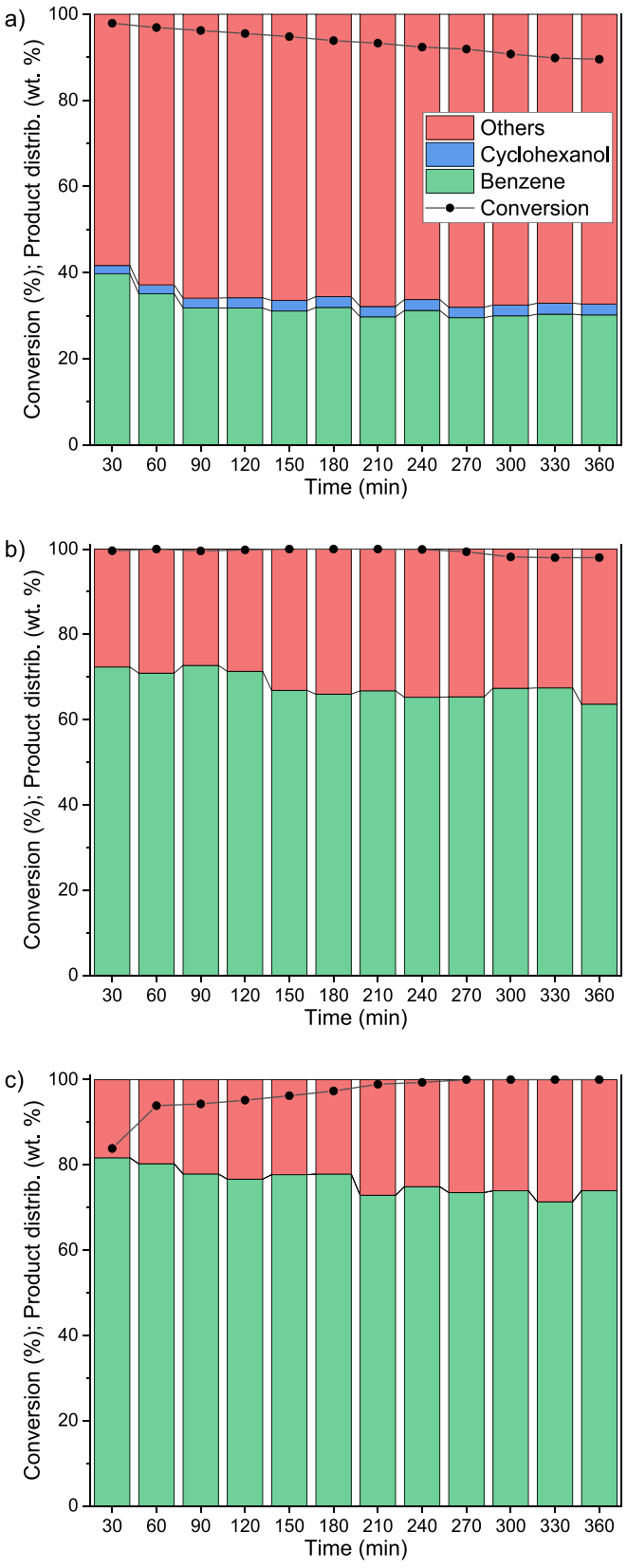

Fig. 4. Conversions and product distribution obtained in the HDO of guaiacol for a WHSV of 4 $g_{org}\ g_{cat}^{-1}\ h^{-1}$, an H_2 pressure of 75 bar and a temperature of a) 300, b) 325 and c) 350 °C.

would become benzene, transforming to cyclohexane after hydrodeoxygenation.

3.4. Evaluation of the catalyst stability

To evaluate the long-term stability of the Mo_2C/CNF catalyst at the more favored conditions (350 °C, 75 bar and 4 $g_{org}\ g_{cat}^{-1}\ h^{-1}$), a 30 h stability test was carried out. As seen in Fig. 5a, the catalyst showed stable behavior during 30 h, which indicates that operational parameters have been set correctly. Additionally, the product distribution is constant with time, with the upgraded bio-oil containing around 80% of the target products.

A catalytic stress test was also carried out to study the stability of the Mo_2C/CNF under non-favorable conditions. To do so, the hourly space velocity was increased from 4 to 10 $g_{org}\ g_{cat}^{-1}\ h^{-1}$, keeping the rest of the parameters at the same values as the stability test previously mentioned. As seen in Fig. 5b, non-favorable conditions led to lower conversion and different product distribution in comparison with Fig. 5a. By comparing the conversion, it can be seen that higher flow rates drop from full range conversion to values between 60 and 40%. Despite this, the conversion keeps floating around 50%, with a slight deactivation over time. Along with this variation in conversion value, the flow rate increment led to a completely different product distribution (Fig. 5b vs. Fig. 5a). The relative amount of "others" rose notably from 20% to around 50% as the benzene content dropped to its lower composition of around 20%. Additionally, the proportion of benzene drops, and there is a rise in the intermediate compounds, such as phenol or cyclohexanol, at the end of the test.

Tran et al. (2019) [61] also varied the space velocity during the HDO of guaiacol in the range of 1.8–39 $g_{guaiacol}g_{cat}^{-1}\ h^{-1}$. They reported that lower space velocities improved the guaiacol conversion and benzene selectivity with a MoWC catalyst. Meanwhile, higher WHSV reduced the guaiacol conversion and increased the presence of phenol in the liquid product. This behavior suggests that in order to deoxygenate the guaiacol molecule fully, lower space velocities are required. However, the operational parameters could be changed into a higher selectivity of benzene or phenol compounds.

In order to gain more insights into the different performance of the catalysts in both operating conditions, they were characterized by XRD and XPS before and after the reaction. As shown in Fig. 6, all catalysts present similar diffractograms and the same crystal phases: Mo_2C and graphite, as well as MoO_2 in very low presence. Based on these results, a high deactivation of the catalyst can be discarded. Although the Mo_2C phase of the catalyst remains after the 30 h tests, slight differences in its

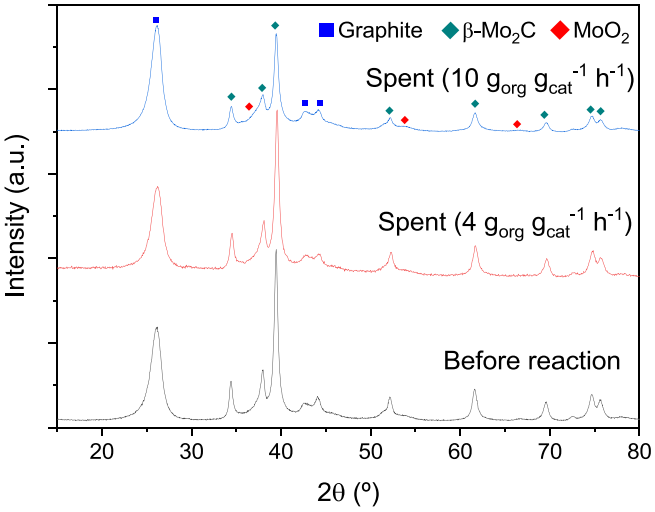

Fig. 6. Diffractograms for catalysts before and after the guaiacol HDO at different WHSV.

intensity are appreciated, with these being related to a slight increase in the crystal size. Under the HDO conditions studied (T = 350 °C; H_2 pressure = 75 bar), the catalyst could be further carboreduced, explaining the slight increase in the Mo_2C crystal size. Likewise, the molybdenum oxide phase is equally insignificant in the catalyst before or after the reaction, regardless of the WHSV used. These results seem to indicate that the catalyst is capable of performing long-lasting tests, throwing high conversion rates and high target product distribution with a slight modification of the molybdenum carbide phase.

The amount of surface Mo was determined by XPS. Unlike XRD, which is a bulk technique, XPS analysis is superficial, so the concentration of Mo oxides in the catalysts is overestimated. It can be observed that the amount of surface Mo is similar to that of the spent catalyst used at a WHSV: 4 $g_{org}\ g_{cat}^{-1}\ h^{-1}$ as compared to the fresh catalyst. However, a significant decrease in the amount of superficial Mo in the catalyst used at a WHSV: 10 $g_{org}\ g_{cat}^{-1}\ h^{-1}$ was observed. This can be tentatively explained by the largest amount of oligomeric species adsorbed on the catalyst surface, thus decreasing the amount of surface Mo available. From XPS, oxidation states were also evaluated, and the following contributions were identified according to the Mo3d region deconvolution (Fig. 7 and Table 1): Mo^{2+} (Mo_2C), $Mo^{\delta+}$, Mo^{4+}(MoO_2) and Mo^{6+} (MoO_3). $Mo^{\delta+}$ state ($2+ < \delta + < 4+$) corresponds to a Mo oxycarbide

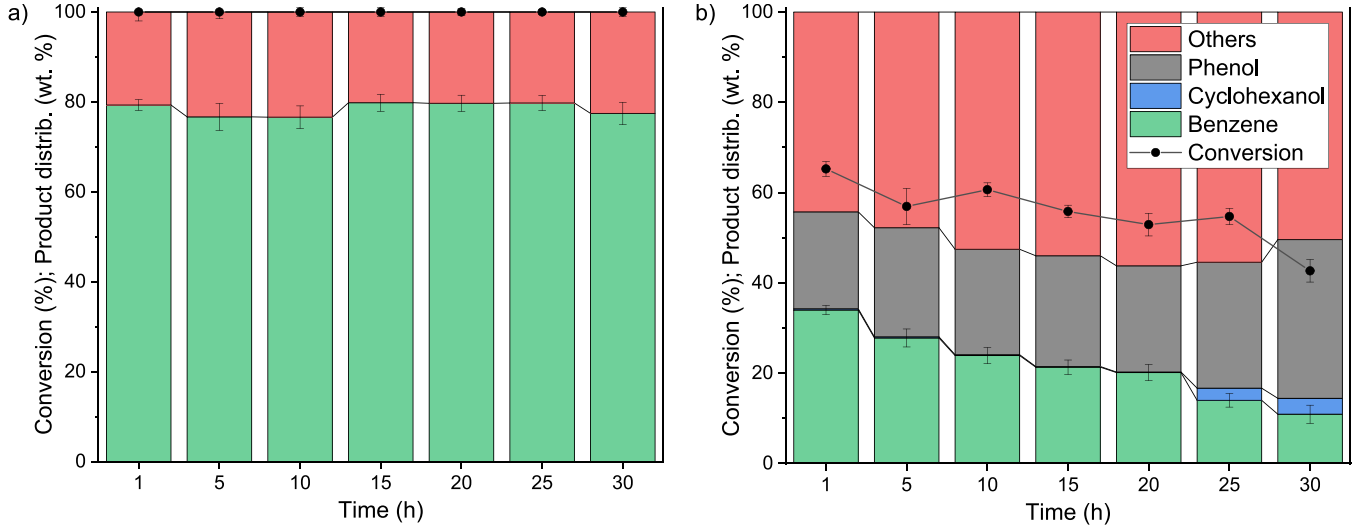

Fig. 5. Stability test results at 350 °C, 75 bar, and WHSV of a) 4 and b) 10 $g_{org}\ g_{cat}^{-1}\ h^{-1}$.

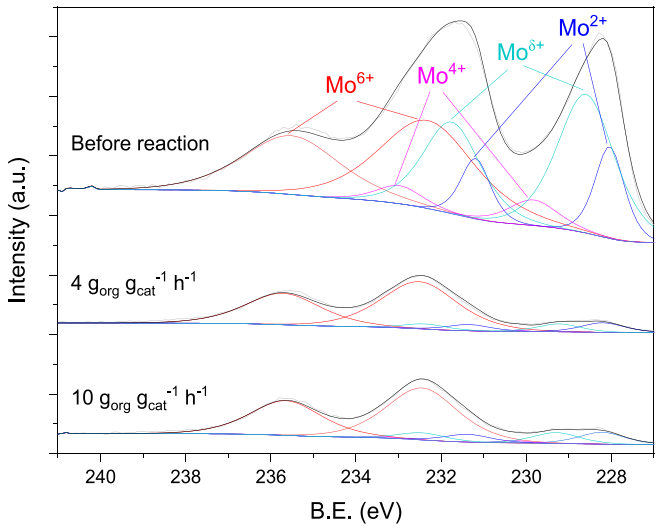

Fig. 7. Deconvolution of the Mo3d XPS region for catalysts before and after stability tests.

Table 1
Crystal size of Mo_2C (XRD) and surface Mo amount and oxidation state (XPS) for catalysts before and after the guaiacol HDO at different WHSV.

	Mo_2C (nm)	Surface Mo (wt%)	Mo^{6+} (at. %)	Mo^{4+} (at. %)	$Mo^{\delta+}$ (at. %)	Mo^{2+} (at. %)
Fresh	12.3	17.5	41.6	6.2	39.0	13.3
Spent (4 $g_{org}\ g_{cat}^{-1}\ h^{-1}$)	17.6	19.2	82.3	0.5	7.7	9.5
Spent (10 $g_{org}\ g_{cat}^{-1}\ h^{-1}$)	14.7	12.9	76.9	1.4	10.4	11.2

phase [65]. No significant differences were observed in the phase distribution (Table 1) in the catalysts used at different WHSV. Nonetheless, an increase in the contribution of oxides (+6) in the spent catalyst after the reaction with respect to the fresh catalyst is observed, which resulted in a decrease in the oxycarbide phase. A plausible explanation for these phenomena is that these oxycarbide species are oxidized by contact with water molecules released during the HDO process. In parallel, the contribution of $Mo^{2}+$ species associated with the carbide phase (Mo_2C) only suffers from a slight decrease compared to the fresh catalyst, regardless of the space velocity used. This indicates that the carbide phase is more resistant to oxidation than the other Mo species, being responsible for the high catalytic stability shown by the Mo_2C/CNF catalyst in the long-term experiments carried out at different space velocities.

4. Conclusions

Hydrodeoxygenation of guaiacol was successfully studied in a continuous trickle-bed reactor using a Mo_2C/CNF-based catalyst, addressing the impact of the hydrogen pressure, reaction temperature and weight hourly space velocity on the process. The experimental results revealed that our Mo_2C/CNF catalyst achieved a conversion as high as 90–98% with a relative amount of benzene in the liquid product up to 81% at 75 bar of H_2 and 350 °C. These excellent results were improved by reducing the weight hourly space velocity from 10 to 4 $g_{org}\ g_{cat}^{-1}\ h^{-1}$, which led to substantial improvements in benzene production (2.4 times compared to a WHSV of 10 $g_{org}\ g_{cat}^{-1}\ h^{-1}$) and catalyst stability, allowing for steady conversions for a period of up to 30 h. Post-mortem analysis of the catalysts revealed the stability of the carbide phase during long-term runs (30*h*), thus explaining the high activity and proportion of benzene in the liquid product.

CRediT authorship contribution statement

J. Gracia: Writing – original draft, Visualization, Investigation, Formal analysis, Data curation. **A. Ayala-Cortés:** Validation, Investigation, Writing – review & editing. **C. Di Stasi:** Writing – review & editing, Writing – original draft, Visualization, Validation, Investigation. **J. Remón:** Validation, Investigation, Writing – review & editing. **D. Torres:** Writing – review & editing, Validation, Investigation. **J.L. Pinilla:** Writing – review & editing, Supervision, Project administration, Methodology, Funding acquisition, Conceptualization. **I. Suelves:** Writing – review & editing, Supervision, Project administration, Methodology, Funding acquisition, Conceptualization.

Declaration of competing interest

The authors declare the following financial interests/personal relationships which may be considered as potential competing interests:

Jose Luis Pinilla reports financial support was provided by State Agency of Research. If there are other authors, they declare that they have no known competing financial interests or personal relationships that could have appeared to influence the work reported in this paper.

Data availability

Data will be made available on request.

Acknowledgments

The authors are grateful for the financial support from the Spanish Ministry of Economy and Competitiveness (MINECO, Project ENE2017-83854-R) and the I + D + i project PID2020-115053RB-I00, funded by MCIN/ AEI/10.13039/501100011033 and by Aragón Government (Research Group Reference T06-23R). J.R., DT and CDS are grateful to the Spanish Ministry of Science, Innovation and Universities for the Juan de la Cierva Incorporación (JdC-I) fellowships (Grant Number: IJC2018-037110-I, IJC2020-045553-I and JDC2022-048765-I, respectively) awarded. J.R. also thanks MCIN/AEI/10.13039/501100011033 and the European Union «NextGenerationEU»/PRTR» for the Ramón y Cajal Fellowship (RYC2021-033368-I) awarded, and the Aragón Government (Research Group Reference T22_23R) for providing frame support. JG is grateful to the Spanish Ministry of Science, Innovation and Universities for his FPI (PRE2018-085182) fellowships.

References

[1] C.-N. Ong, B.-L. Lee, Determination of benzene and its metabolites: application in biological monitoring of environmental and occupational exposure to benzene, J. Chromatogr. B Biomed. Sci. Appl. 660 (1994) 1–22, https://doi.org/10.1016/0378-4347(94)00278-9.
[2] J.C. Gentry, Benzene production and economics: a review, Asia Pac. J. Chem. Eng. 2 (2007) 272–277, https://doi.org/10.1002/apj.18.
[3] J.P. Garcia Villaluenga, A. Tabe-Mohammadi, A review on the separation of benzene/cyclohexane mixtures by pervaporation processes, J. Membr. Sci. 169 (2000) 159–174, https://doi.org/10.1016/S0376-7388(99)00337-3.
[4] P. Kumar, S.R. Yenumala, S.K. Maity, D. Shee, Kinetics of hydrodeoxygenation of stearic acid using supported nickel catalysts: effects of supports, Appl. Catal. A Gen. 471 (2014) 28–38, https://doi.org/10.1016/j.apcata.2013.11.021.
[5] A. Demirbas, Political, economic and environmental impacts of biofuels: a review, Appl. Energy 86 (2009) S108–S117, https://doi.org/10.1016/j.apenergy.2009.04.036.
[6] L. Zhang, C. Xu, P. Champagne, Overview of recent advances in thermo-chemical conversion of biomass, Energy Convers. Manag. 51 (2010) 969–982, https://doi.org/10.1016/j.enconman.2009.11.038.
[7] M. Fatih Demirbas, Biorefineries for biofuel upgrading: a critical review, Appl. Energy 86 (2009) S151–S161, https://doi.org/10.1016/j.apenergy.2009.04.043.
[8] M. Ni, D.Y.C. Leung, M.K.H. Leung, K. Sumathy, An overview of hydrogen production from biomass, Fuel Process. Technol. 87 (2006) 461–472, https://doi.org/10.1016/j.fuproc.2005.11.003.
[9] C. Di Stasi, G. Greco, R.L.S. Canevesi, M.T. Izquierdo, V. Fierro, A. Celzard, B. González, J.J. Manyà, Influence of activation conditions on textural properties

and performance of activated biochars for pyrolysis vapors upgrading, Fuel 289 (2021) 119759, https://doi.org/10.1016/j.fuel.2020.119759.
[10] C. Di Stasi, M. Cortese, G. Greco, S. Renda, B. González, V. Palma, J.J. Manyà, Optimization of the operating conditions for steam reforming of slow pyrolysis oil over an activated biochar-supported Ni–Co catalyst, Int. J. Hydrog. Energy 46 (2021) 26915–26929, https://doi.org/10.1016/j.ijhydene.2021.05.193.
[11] C. Di Stasi, D. Alvira, G. Greco, B. González, J.J. Manyà, Physically activated wheat straw-derived biochar for biomass pyrolysis vapors upgrading with high resistance against coke deactivation, Fuel 255 (2019) 115807, https://doi.org/10.1016/j.fuel.2019.115807.
[12] A.R.K. Gollakota, C.-M. Shu, P.K. Sarangi, K.P. Shadangi, S. Rakshit, J.F. Kennedy, V.K. Gupta, M. Sharma, Catalytic hydrodeoxygenation of bio-oil and model compounds – choice of catalysts, and mechanisms, Renew. Sust. Energ. Rev. 187 (2023) 113700, https://doi.org/10.1016/j.rser.2023.113700.
[13] G.W. Huber, S. Iborra, A. Corma, Synthesis of transportation fuels from biomass: chemistry, catalysts, and engineering, Chem. Rev. 106 (2006) 4044–4098, https://doi.org/10.1021/cr068360d.
[14] N. Arun, R.V. Sharma, A.K. Dalai, Green diesel synthesis by hydrodeoxygenation of bio-based feedstocks: strategies for catalyst design and development, Renew. Sust. Energ. Rev. 48 (2015) 240–255, https://doi.org/10.1016/j.rser.2015.03.074.
[15] Q. Lu, W.-Z. Li, X.-F. Zhu, Overview of fuel properties of biomass fast pyrolysis oils, Energy Convers. Manag. 50 (2009) 1376–1383, https://doi.org/10.1016/j.enconman.2009.01.001.
[16] D. Carpenter, T.L. Westover, S. Czernik, W. Jablonski, Biomass feedstocks for renewable fuel production: a review of the impacts of feedstock and pretreatment on the yield and product distribution of fast pyrolysis bio-oils and vapors, Green Chem. 16 (2014) 384–406, https://doi.org/10.1039/C3GC41631C.
[17] C. Muangsuwan, W. Kriprasertkul, S. Ratchahat, C.-G. Liu, P. Posoknistakul, N. Laosiripojana, C. Sakdaronnarong, Upgrading of light bio-oil from solvothermolysis liquefaction of an oil palm empty fruit bunch in glycerol by catalytic hydrodeoxygenation using NiMo/Al2O3 or CoMo/Al2O3 catalysts, ACS Omega 6 (2021) 2999–3016, https://doi.org/10.1021/acsomega.0c05387.
[18] T.V. Choudhary, C.B. Phillips, Renewable fuels via catalytic hydrodeoxygenation, Appl. Catal. A Gen. 397 (2011) 1–12, https://doi.org/10.1016/j.apcata.2011.02.025.
[19] H. Wang, M. Feng, B. Yang, Catalytic hydrodeoxygenation of anisole: an insight into the role of metals in transalkylation reactions in bio-oil upgrading, Green Chem. 19 (2017) 1668–1673, https://doi.org/10.1039/c6gc03198f.
[20] B. Valle, A. Remiro, N. García-Gómez, A.G. Gayubo, J. Bilbao, Recent research progress on bio-oil conversion into bio-fuels and raw chemicals: a review, J. Chem. Technol. Biotechnol. 94 (2019) 670–689, https://doi.org/10.1002/jctb.5758.
[21] Z. Si, X. Zhang, C. Wang, L. Ma, R. Dong, An overview on catalytic hydrodeoxygenation of pyrolysis oil and its model compounds, Catalysts 7 (2017) 169, https://doi.org/10.3390/catal7060169.
[22] V.S. Prabhudesai, L. Gurrala, R. Vinu, Catalytic hydrodeoxygenation of lignin-derived oxygenates: catalysis, mechanism, and effect of process conditions, Energy Fuel 36 (2022) 1155–1188, https://doi.org/10.1021/acs.energyfuels.1c02640.
[23] L. Qu, X. Jiang, Z. Zhang, X.-g. Zhang, G.-y. Song, H.-l. Wang, Y.-p. Yuan, Y.-l. Chang, A review of hydrodeoxygenation of bio-oil: model compounds, catalysts, and equipment, Green Chem. 23 (2021) 9348–9376, https://doi.org/10.1039/D1GC03183J.
[24] H.Y. Zhao, D. Li, P. Bui, S.T. Oyama, Hydrodeoxygenation of guaiacol as model compound for pyrolysis oil on transition metal phosphide hydroprocessing catalysts, Appl. Catal. A Gen. 391 (2011) 305–310, https://doi.org/10.1016/j.apcata.2010.07.039.
[25] V.N. Bui, D. Laurenti, P. Afanasiev, C. Geantet, Hydrodeoxygenation of guaiacol with CoMo catalysts. Part I: promoting effect of cobalt on HDO selectivity and activity, Appl. Catal. B Environ. 101 (2011) 239–245, https://doi.org/10.1016/j.apcatb.2010.10.025.
[26] C.R. Lee, J.S. Yoon, Y.-W. Suh, J.-W. Choi, J.-M. Ha, D.J. Suh, Y.-K. Park, Catalytic roles of metals and supports on hydrodeoxygenation of lignin monomer guaiacol, Catal. Commun. 17 (2012) 54–58, https://doi.org/10.1016/j.catcom.2011.10.011.
[27] E.H. Lee, R.-s. Park, H. Kim, S.H. Park, S.-C. Jung, J.-K. Jeon, S.C. Kim, Y.-K. Park, Hydrodeoxygenation of guaiacol over Pt loaded zeolitic materials, J. Ind. Eng. Chem. 37 (2016) 18–21, https://doi.org/10.1016/j.jiec.2016.03.019.
[28] G.-H. Han, M.W. Lee, S. Park, H.J. Kim, J.-P. Ahn, M.-g. Seo, K.-Y. Lee, Revealing the factors determining the selectivity of guaiacol HDO reaction pathways using ZrP-supported Co and Ni catalysts, J. Catal. 377 (2019) 343–357, https://doi.org/10.1016/j.jcat.2019.07.034.
[29] N.B. Van, D. Laurenti, P. Delichere, C. Geantet, Hydrodeoxygenation of guaiacol Part II: support effect for CoMoS catalysts on HDO activity and selectivity, Appl. Catal. B Environ. 101 (2011) 246–255, https://doi.org/10.1016/j.apcatb.2010.10.031.
[30] X. Li, G. Chen, C. Liu, W. Ma, B. Yan, J. Zhang, Hydrodeoxygenation of lignin-derived bio-oil using molecular sieves supported metal catalysts: a critical review, Renew. Sust. Energ. Rev. 71 (2017) 296–308, https://doi.org/10.1016/j.rser.2016.12.057.
[31] P.M. Mortensen, J.D. Grunwaldt, P.A. Jensen, K.G. Knudsen, A.D. Jensen, A review of catalytic upgrading of bio-oil to engine fuels, Appl. Catal. A Gen. 407 (2011) 1–19, https://doi.org/10.1016/j.apcata.2011.08.046.
[32] E. Furimsky, Metal carbides and nitrides as potential catalysts for hydroprocessing, Appl. Catal. A Gen. 240 (2003) 1–28, https://doi.org/10.1016/S0926-860X(02)00428-3.
[33] Y. Ma, G. Guan, X. Hao, J. Cao, A. Abudula, Molybdenum carbide as alternative catalyst for hydrogen production – a review, Renew. Sust. Energ. Rev. 75 (2017) 1101–1129, https://doi.org/10.1016/j.rser.2016.11.092.
[34] M. Führer, T. Van Haasterecht, J. Bitter, Molybdenum and tungsten carbides can shine too, Catal. Sci. Technol. 10 (2020) 6089–6097, https://doi.org/10.1039/D0CY01420F.
[35] A. Gutierrez, R.K. Kaila, M.L. Honkela, R. Slioor, A.O.I. Krause, Hydrodeoxygenation of guaiacol on noble metal catalysts, Catal. Today 147 (2009) 239–246, https://doi.org/10.1016/j.cattod.2008.10.037.
[36] Y. Deng, Y. Ge, M. Xu, Q. Yu, D. Xiao, S. Yao, D. Ma, Molybdenum carbide: controlling the geometric and electronic structure of noble metals for the activation of O–H and C–H bonds, Acc. Chem. Res. 52 (2019) 3372–3383, https://doi.org/10.1021/acs.accounts.9b00182.
[37] S.A. Rasaki, B. Zhang, K. Anbalgam, T. Thomas, M. Yang, Synthesis and application of nano-structured metal nitrides and carbides: a review, Prog. Solid State Chem. 50 (2018) 1–15, https://doi.org/10.1016/j.progsolidstchem.2018.05.001.
[38] Z. Lin, R. Chen, Z. Qu, J.G. Chen, Hydrodeoxygenation of biomass-derived oxygenates over metal carbides: from model surfaces to powder catalysts, Green Chem. 20 (2018) 2679–2696, https://doi.org/10.1039/C8GC00239H.
[39] N. Tran, Y. Uemura, T. Trinh, A. Ramli, Hydrodeoxygenation of guaiacol over Pd–Co and Pd–Fe catalysts: deactivation and regeneration, Processes 9 (2021) 430, https://doi.org/10.3390/pr9030430.
[40] D. Gao, C. Schweitzer, H.T. Hwang, A. Varma, Conversion of guaiacol on noble metal catalysts: reaction performance and deactivation studies, Ind. Eng. Chem. Res. 53 (2014) 18658–18667, https://doi.org/10.1021/ie500495z.
[41] R.F. Nunes, D. Costa, A.M. Ferraria, A.M. Botelho do Rego, F. Ribeiro, Â. Martins, A. Fernandes, Heterogenization of heteropolyacid with metal-based alumina supports for the guaiacol gas-phase hydrodeoxygenation, Molecules 28 (2023) 2245, https://doi.org/10.3390/molecules28052245.
[42] M. Führer, T. van Haasterecht, J.H. Bitter, Catalytic performance of carbon-supported mixed MoW carbides for the deoxygenation of stearic acid, Catal. Today 418 (2023) 114108, https://doi.org/10.1016/j.cattod.2023.114108.
[43] E. Santillan-Jimenez, M. Perdu, R. Pace, T. Morgan, M. Crocker, Activated carbon, carbon nanofiber and carbon nanotube supported molybdenum carbide catalysts for the hydrodeoxygenation of guaiacol, Catalysts (2015) 424–441.
[44] E. Ochoa, D. Torres, R. Moreira, J.L. Pinilla, I. Suelves, Carbon nanofiber supported Mo2C catalysts for hydrodeoxygenation of guaiacol: the importance of the carburization process, Appl. Catal. B Environ. 239 (2018) 463–474, https://doi.org/10.1016/j.apcatb.2018.08.043.
[45] E. Ochoa, D. Torres, J.L. Pinilla, I. Suelves, Nanostructured carbon material effect on the synthesis of carbon-supported molybdenum carbide catalysts for guaiacol hydrodeoxygenation, Energies 13 (5) (2020) 1189–1208.
[46] H. Yang, X. Zhu, H.W. Amini, B. Fachri, M. Ahmadi, G.H. ten Brink, P.J. Deuss, H. J. Heeres, Efficient Cu-based catalysts for the selective demethoxylation of guaiacols, Appl. Catal. A Gen. 654 (2023) 119062, https://doi.org/10.1016/j.apcata.2023.119062.
[47] M. Schmal, R.W.S. Lima, T.L.R. Hewer, R.M.B. Alves, Hydrodeoxygenation (HDO + HDA) of guaiacol, anisole and a mixture on Ni-Mo catalysts supported on SBA-15 and γ-Al2O3, Braz. J. Chem. Eng. (2023), https://doi.org/10.1007/s43153-023-00344-9.
[48] F.G. Baddour, V.A. Witte, C.P. Nash, M.B. Griffin, D.A. Ruddy, J.A. Schaidle, Late-transition-metal-modified β-Mo2C catalysts for enhanced hydrogenation during guaiacol deoxygenation, ACS Sustain. Chem. Eng. 5 (2017) 11433–11439, https://doi.org/10.1021/acssuschemeng.7b02544.
[49] Z. Yu, Z. Yu, Y. Wang, Z. Sun, Y. Liu, A. Wang, Hydrodeoxygenation of guaiacol to aromatic hydrocarbons over Mo2C prepared in nonthermal plasma, Plasma Chem. Plasma Process. 42 (2022) 1069–1083, https://doi.org/10.1007/s11090-022-10257-z.
[50] C.-C. Tran, O. Mohan, A. Banerjee, S.H. Mushrif, S. Kaliaguine, A combined experimental and DFT investigation of selective hydrodeoxygenation of guaiacol over bimetallic carbides, Energy Fuel 34 (2020) 16265–16273, https://doi.org/10.1021/acs.energyfuels.0c03102.
[51] E. Ochoa, D. Torres, J. Pinilla, I. Suelves, Influence of carburization time on the activity of Mo2C/CNF catalysts for the HDO of guaiacol, Catal. Today 357 (2020) 240–247.
[52] J. Pinilla, S. De Llobet, R. Moliner, I. Suelves, Ni-Co bimetallic catalysts for the simultaneous production of carbon nanofibres and syngas through biogas decomposition, Appl. Catal. B Environ. 200 (2017) 255–264.
[53] J. Remón, E. Ochoa, C. Foguet, J.L. Pinilla, I. Suelves, Towards a sustainable bio-fuels production from lignocellulosic bio-oils: Influence of operating conditions on the hydrodeoxygenation of guaiacol over a Mo2C/CNF catalyst, Fuel Process. Technol. 191 (2019) 111–120, https://doi.org/10.1016/j.fuproc.2019.04.008.
[54] A. Ayala-Cortés, D. Torres, E. Frecha, P. Arcelus-Arrillaga, H.I. Villafán-Vidales, A. Longoria, J.L. Pinilla, I. Suelves, Catalytic hydrodeoxygenation of solar energy produced bio-oil in supercritical ethanol with Mo2C/CNF catalysts: effect of mo concentration, Catalysts 13 (12) (2023) 1500–1518.
[55] R. Moreira, E. Ochoa, J.L. Pinilla, A. Portugal, I. Suelves, Liquid-phase hydrodeoxygenation of guaiacol over Mo2C supported on commercial CNF. Effects of operating conditions on conversion and product selectivity, Catalysts 8 (4) (2018) 127–141.
[56] M.D. Argyle, C.H. Bartholomew, Heterogeneous catalyst deactivation and regeneration: a review, Catalysts (2015) 145–269.
[57] J.S. Lee, S.T. Oyama, M. Boudart, Molybdenum carbide catalysts: I. Synthesis of unsupported powders, J. Catal. 106 (1987) 125–133, https://doi.org/10.1016/0021-9517(87)90218-1.
[58] D.E. Resasco, S.P. Crossley, Implementation of concepts derived from model compound studies in the separation and conversion of bio-oil to fuel, Catal. Today 257 (2015) 185–199, https://doi.org/10.1016/j.cattod.2014.06.037.

[59] S. Liu, H. Wang, K.J. Smith, C.S. Kim, Hydrodeoxygenation of 2-methoxyphenol over Ru, Pd, and Mo2C catalysts supported on carbon, Energy Fuel 31 (2017) 6378–6388, https://doi.org/10.1021/acs.energyfuels.7b00452.
[60] J.A. Schaidle, J. Blackburn, C.A. Farberow, C. Nash, K.X. Steirer, J. Clark, D. J. Robichaud, D.A. Ruddy, Experimental and computational investigation of acetic acid deoxygenation over oxophilic molybdenum carbide: surface chemistry and active site identity, ACS Catal. 6 (2016) 1181–1197, https://doi.org/10.1021/acscatal.5b01930.
[61] C.C. Tran, Y. Han, M. Garcia-Perez, S. Kaliaguine, Synergistic effect of Mo-W carbides on selective hydrodeoxygenation of guaiacol to oxygen-free aromatic hydrocarbons, Catal. Sci. Technol. 9 (2019) 1387–1397, https://doi.org/10.1039/c8cy02184h.
[62] Y.C. Lin, C.L. Li, H.P. Wan, H.T. Lee, C.F. Liu, Catalytic hydrodeoxygenation of guaiacol on Rh-based and sulfided CoMo and NiMo catalysts, Energy Fuel 25 (2011) 890–896, https://doi.org/10.1021/ef101521z.
[63] Y. Wu, X. Xu, Y. Sun, E. Jiang, X. Fan, R. Tu, J. Wang, Gas-phase hydrodeoxygenation of guaiacol over Ni-based HUSY zeolite catalysts under atmospheric H2 pressure, Renew. Energy 152 (2020) 1380–1390, https://doi.org/10.1016/j.renene.2020.01.117.
[64] C.J. Chen, W.S. Lee, A. Bhan, Mo2C catalyzed vapor phase hydrodeoxygenation of lignin-derived phenolic compound mixtures to aromatics under ambient pressure, Appl. Catal. A Gen. 510 (2016) 42–48, https://doi.org/10.1016/j.apcata.2015.10.043.
[65] H. Wang, S. Liu, K.J. Smith, Synthesis and hydrodeoxygenation activity of carbon supported molybdenum carbide and oxycarbide catalysts, Energy Fuel 30 (2016) 6039–6049, https://doi.org/10.1021/acs.energyfuels.6b01032.